

DEVELOPMENT OF THE TECHNOLOGY OF MANUFACTURING DOUBLE-WALL WELDED TRANSFORMABLE-SHELL STRUCTURE

L.M. LOBANOV and V.S. VOLKOV

E.O. Paton Electric Welding Institute, NASU, Kiev, Ukraine

Transformable-shell structures (TSS) of a conical type are considered, which are a unique development of PWI, and have no foreign analogs. Engineering solutions are proposed which allow improvement of reliability of shell TSS, as well as technological approaches to their realization. A brief description of the technology of producing permanent joints on sheets of austenitic stainless steel, capable of ensuring the leak-tightness of deformed shells, is given.

Keywords: transformable-shell structures, load-carrying shells, double-wall transformable shells

At development of shell structures one of the most urgent problems is ensuring their service properties – leak-tightness and fatigue life, strength and corrosion resistance of welded joints. In transformable-shell structures (TSS) developed at PWI, the reliability of welds and material of the shell are particularly important, as they undergo considerable bending during transformation, reaching 150° in the vortices of technological corrugations [1]. Promising applications of TSS as storage tanks for bulk and liquid materials, including substances with increased reactivity, require looking for effective methods to improve the shell reliability. The most rational solution can be development of a two-layer struc-

ture, in which outer wall duplication with separation of its enclosing and load-carrying functions can prevent the consequences of possible loss of tightness.

In most of the cases, technology of TSS manufacturing by forming corrugated discs from thin-walled conical shells is preferable, allowing fabrication of structures of a broad range of typesizes and parameters. Isometric transformation of a closed shell in the form of a truncated cone can be realized by dissection of its surface by a family of planes, normal to cone axis, and successive mirror reflection of the parts of the surface relative to the respective planes $\gamma_n, \gamma_{n+1}, \dots, \gamma_k$ (Figure 1). At crossing of the transformed Q_{n+1} and untransformed Q_n parts of the surface a rib is formed in the crossing region, which lies in plane γ_n and moves together with it during transformation. The essence of the method developed at PWI consists in successive, close to an isometric one, bending of a smooth conical blank and forming a corrugated disc by local impact of the forming tool on a rotating shell [2]. The bent circular area of the blank encloses the tool working surface, moves from the outer part of its side surface to the inner side, and takes a position, which is a mirror reflection of the initial one, forming the inner wall of the circular corrugation. The corrugation outer wall is formed by an undeformed section of the shell, which moves along its axis of rotation. During forming of each subsequent corrugation of depth k the height of the conical shell decreases by a value equal to $2k$. Simultaneous forming of two conical shells Q and \bar{Q} in one technological process allows creating topologically equivalent corrugated surfaces Q_1, \bar{Q}_1 , superposable by moving along the axis of symmetry.

Optimum modes of forming two-layer corrugated discs by bending shells of 12Kh18N10T stainless steel with outer diameter $D = 150$ mm

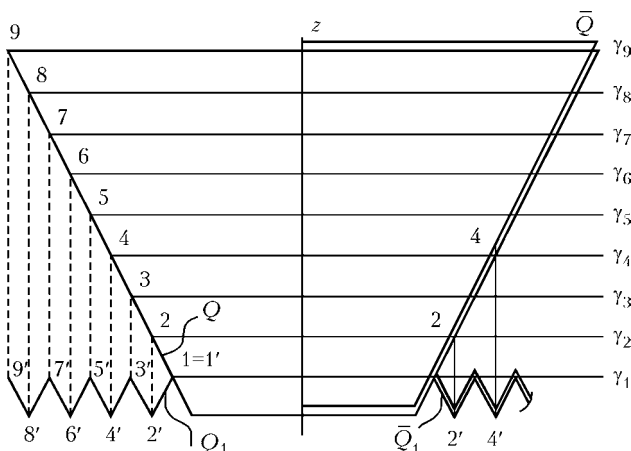


Figure 1. Schematic of isometric transformation of closed conical shells: γ_1 – γ_9 – parallel secant planes; 1–9 – points of intersection of secant plane traces with side generatrix of the conical surface; 1'–9' – points of reflected part of the surface corresponding to points 1–9; Q, Q_1 and \bar{Q}, \bar{Q}_1 – untransformed and transformed parts of the circular cone surface

Microplasma welding modes studied

Strip thickness, mm	Welding current, A	Welding voltage, V	Welding speed, cm/s	Shielding atmosphere	Results		
					Weld width, mm	Lack-of-penetration	Deplanation, mm
0.15	3.5	10	0.14	Helium	1.35–1.40	Complete	0.45–0.50
0.15	5	10	0.28		1.2–1.3		0.5–0.6
0.15	7	10	0.42		1.4–1.5		0.30–0.35
0.15	8.5	10	0.55		1.3–1.4		0.2–0.3

and wall thickness of 0.15 mm were determined experimentally; one of the conical shells is tightly inserted into the other, which is followed by fixing both the blanks in the centering conical opening of the die-mold. At optimum technological parameters of the process, the produced discs do not have any surface defects with a close contact between the shell layers without any tendency to their subsequent separation: range of speeds of blank rotation at rotational extrusion in the mould is within 50–250 rpm, the speed of forward feed of the forming tool being from 0.3 up to 2.0 mm/rev.

Anticipated applications of conical TSS require paying special attention to working-out the problems of reliability and fatigue life of thin shells, the assembly of which implies presence of extended precise welds. Certain difficulties arise at subsequent welding of two-layer shells around circular contours. Despite tight contact of shell edges in assembly, the gap between the layers increases under the impact of welding heat, that may lead to their lack-of-fusion. Analysis of the currently available welding processes and evaluation of their adaptability to fabrication show that:

- in overlap welding by roll-seam welding machine the joints are 2 times thicker than the base metal. The weld has low ductility properties, its making requires complex fixtures, and the rollers burn on longer welds, thus leading to an increase of contact resistance and deterioration of welded joint quality;
- in microplasma fusion welding uniform high-quality joints are made, no sophisticated equipment or devices are required. With this process a molten metal pool of 0.12–0.17 mm³ volume forms in sheet welding. The smallest disturbances lead to its rupture, i.e. burning-through; this can be avoided by an accurate following of the conditions of assembly and welding; studied parameters of welding modes are given in the Table. Proceeding from investigation results, it is possible to select a mode for specific conditions;
- laser welding requires sophisticated and costly equipment and precision assembly of the

shell sections being welded, that involves considerable difficulties; more over, provision of protection of the molten zone and cooling weld zone is complicated. Nonetheless, this process allows achieving a high quality of welds at their minimum width that is important for sound formation of corrugated discs from the welded shells. In welding by a fiber-optic laser with laser beam power $P = 65$ W of blanks from a steel strip of 12Kh18N10T grade, similar to samples from the Table, at speed $v_w = 2$ cm/s, weld width was equal to $w_w = 0.6–0.7$ mm at complete penetration and deplanation within 0.15–0.25 mm (shielding atmospheres: helium on top and argon from below the weld) [3].

Duration of welding the butt joints in fabrication of TSS of a conical type and relatively high fraction of intermediate assembly operations at other conditions being equal, do not allow regarding welding process speed as the decisive factor, determining the advantage of one of the considered processes. Under the conditions of difficult access to the weld root and complexity of butt aligning at assembly of two shells on load-carrying elements, microplasma process is preferable in most of the cases. Laser welding can be regarded as optimum at the stage of manufacturing the initial conical blanks of corrugated discs, requiring minimum distortions of the surface, when making narrow linear welds with low specific heat input.

At mechanical testing of the studied samples, the nature of deformations of each type of welds, used in TSS linear and circumferential joints, was simulated. To check the strength and ductility characteristics of microplasma welded joints, three standard samples for tensile and bend testing were prepared from each weld. Test results showed that none of the samples failed in the welded joint; rupture passed through the base metal at an angle to sample axis. Sample tension diagram is standard, with a pronounced yield plateau, characteristic for the used steel grade. Produced characteristics (12Kh18N10T steel), depending on thickness h , have the following form:

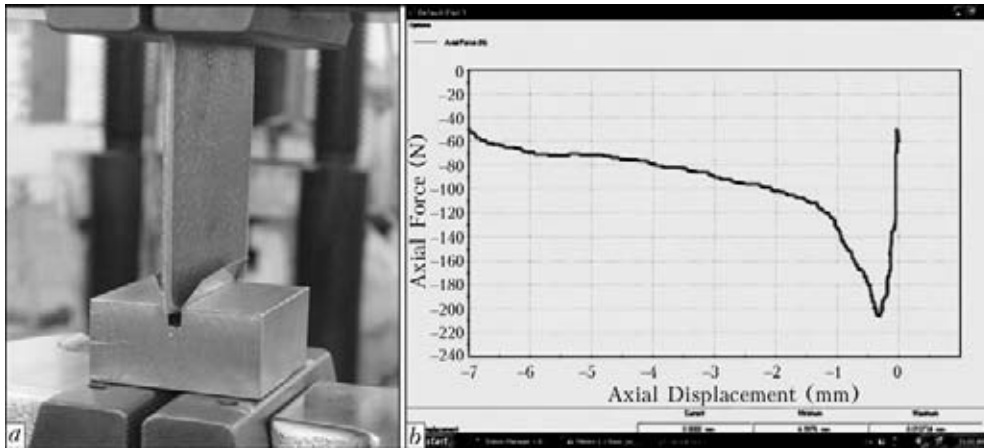


Figure 2. Segment of forming matrix for bend testing of weld fragment (a), and diagram of deformation of 0.15 mm thick sample (b): along ordinate axis – forming force $P_{max} = 230$ N

- for $h = 0.15$ mm
 $\sigma_y = 320\text{--}330$ MPa; $\sigma_t = 68\text{--}71$ MPa;
 $\delta = 40\text{--}42$ %; $\psi = 50\text{--}52$ %;
- for $h = 0.1$ mm
 $\sigma_y = 350\text{--}370$ MPa; $\sigma_t = 70\text{--}72$ MPa;
 $\delta = 39\text{--}41$ %; $\psi = 48\text{--}51$ %.

All the samples were tested for bending up to the angle of 180° in a mandrel with a radius equal to two base metal thicknesses, and no failures or cracks were found. To make testing conditions more complicated, the flattening method was used, in which bending of the rectangular sample was conducted up to touching of its opposite edges; in this case, slight plastic deformation was observed on the weld surface without any indications of welded joint fracture. Thus, strength and ductility of the produced welded joints are not inferior to similar characteristics of the base metal and allow performing the form change of the transformable shells, envisaged by the technology, without violation of their leak-tightness.

Strength tests of butt welded joints of 12Kh18N10T strip, made by laser welding, were conducted in MTS 318.25 testing system in a device, which is a segment of the rotational moulding equipment (matrix) in the area of forming the corrugation with maximum diameter and die with the working edge shape corresponding to the profile of forming roller for this material thickness (Figure 2, a). Figure 2, b shows the deformation diagram obtained at back bending of 0.15 mm thick sample along an axis normal to the weld line. At repeated deformation of each of the three tested samples the curves of $P(l)$ dependence are characterized by shifting of point P_{max} towards the initial values of axial displacements l . After three complete cycles of bending through 180° angle all the samples were examined by liquid-penetrant testing using MR[®] 68 penetrant and MR[®] 70 developer produced by MR[®]

Chemie GmbH with no crack opening or cracks found.

Sealing of the formed corrugated discs was performed by their welding to flat covers of 12Kh18N10T steel around the butt of the small circular contour in the profiled mandrel, ensuring a tight contact of the edges of aligned sections of conical surfaces of the blanks and heat removal in welding of the circumferential weld (Figure 3, a). Technology was verified on shells of larger diameter $D = 140$ mm, smaller diameter $d = 90$ mm, and 0.15 mm thickness as-assembled with covers of design thickness 0.3 mm, and welding was performed without filler material in the automatic mode using microplasma torch with a system of positioning along weld axis and with quality control of welded joint. Welding mode was as follows: $I_w = 3.5$ A, $U = 10$ V, $v_w = 0.33$ cm/s.

Speed of welding by the microplasma torch at disc joining was set by structure rotation in a special fixture. Welded joint quality was controlled visually, and also excess pressure $P = (0.2\text{--}0.3) \cdot 10^{-2}$ MPa was created in the shell inner cavity, with subsequent monitoring of its drop during the next 60 min.

At assembly of corrugated discs on circular load-carrying elements (frame rings) it will be necessary to maintain the relationships of their reciprocal geometrical parameters at all the stages of transformation, which ensure free movement of the inner shell with air compression in the interwall space (caisson) up to a certain pressure, which, in its turn, allows performing complete transformation of the outer shell to design dimensions. Width g of horizontal rims of a frame ring of Π -shaped configuration (Figure 3, c) is determined by the technology of welding along the edge flanges of circumferential contours of the two shells, and is in the range of $g = 40\text{--}50\Delta$, where Δ is the thickness of structural material

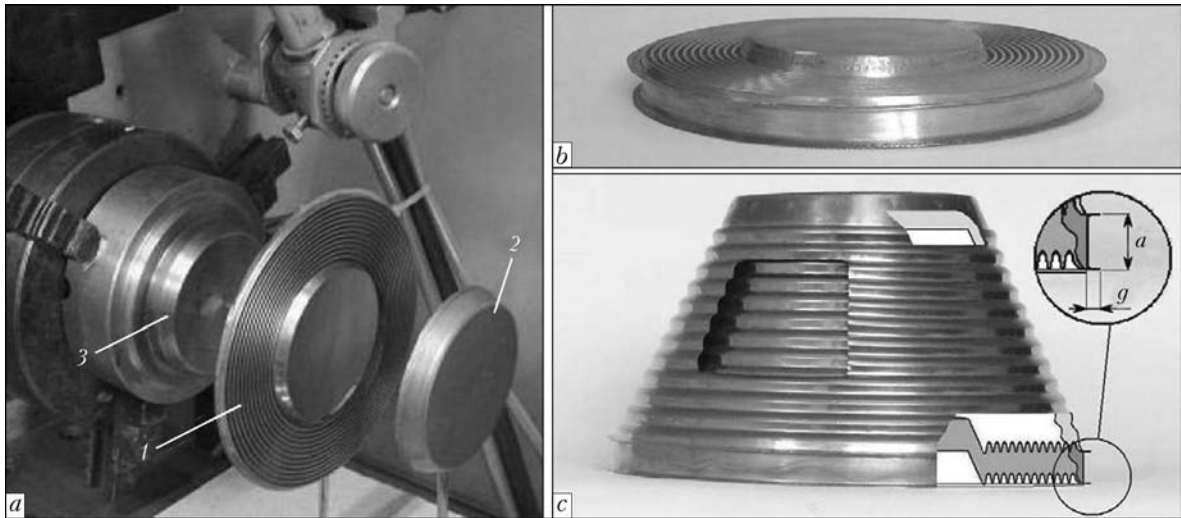


Figure 3. Assembly of initial corrugated discs of double-wall conical shell (a) (1 – corrugated disc; 2 – sealing cover; 3 – profiled mandrel), double-wall TSS with base radii $R = 70$ mm, $r = 49$ mm and angle of conicity $\alpha = 25^\circ$ in the compact (folded) state (b), and the same structure in the deployed state (c); the initial and final phases of transformation are shown in the sectional view on the right (a – frame ring height; g – width of frame ring horizontal rims)

shells; frame ring wall thickness is calculated allowing for process and service loads applied to the structure. Frame ring height a should provide the possibility of simultaneous motion of the shells without contact of any points of their surface.

The process of shell deployment starts with the maximum diameter corrugation. Experimentally derived value of excess pressure, which is necessary for complete deployment of single-wall shell of the studied structure, is equal to 10^5 Pa [4], and is approximately equal to the value of normal atmospheric pressure. Thus, a mandatory condition of complete deployment of the outer shell is 2 times increase of initial air pressure P_1 in the interwall caisson at drawing together of shells at all the transformation stages $P_2 = 2P_1$. Therefore, at isothermal compression of air $V_2 = V_1/2$, where V_1, V_2 are the caisson volumes at the initial moment of deployment of inner shell corrugation and at the initial moment of deployment of the corresponding outer corrugation. However, as follows from the condition of pres-

ervation of isometricity S_1 and S_2 , at the final stage of transformation volumes V_1, V_2 and pressures P_1 and P_2 , respectively, are equal, that means the impossibility of complete deployment of the last corrugation n_i of minimum diameter. In addition, required $P_2 = 2P_1$ ratio at forming of corrugation n_1 of maximum diameter corresponds to condition $l = a/2$, and for the next corrugations parameter l grows because of the change of the volume ratio of transformed and untransformed sections of interwall caisson that may lead to mechanical contact of the shells in the region of minimum diameter corrugations, local loss of stability and distortion of their surfaces. Therefore, frame ring height a is selected proceeding from the condition $a \geq k$, where k is the depth of corrugation forming; maximum a values are limited by the requirements of structure compactness, and, therefore increase of its transformation coefficient.

Figure 4, b gives a schematic of transformation of the last corrugation of the shells, which is of

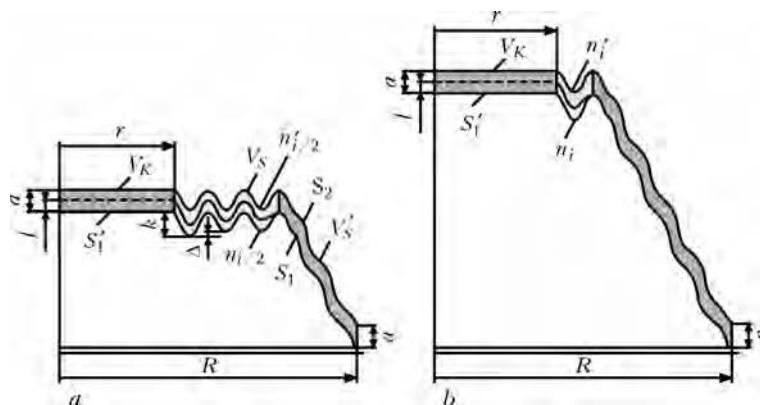


Figure 4. Schematic of transformation of corrugations of double-wall TSS with medium $n_{i/2}$ (a) and minimum n_i (b) diameters

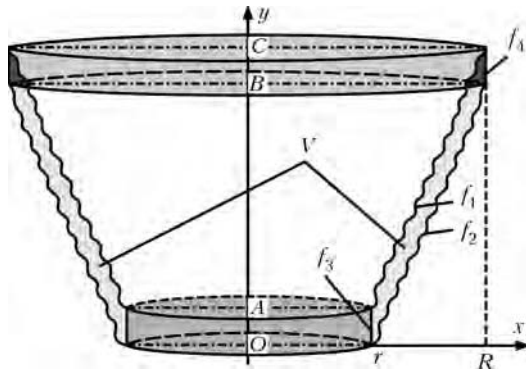


Figure 5. Schematic of double-wall TSS

minimum diameter. Interwall space V is divided into three conditional volumes, with their ratios changing continuously during structure deployment: V_K , limited by sealing covers; V'_S and V_S , limited by transformed and untransformed sections of side corrugated surfaces, respectively. At $l \approx a$ pressure of deployment of corrugation $n_i P_2 = P_1 V_1 / V_2$ and $V_1 / V_2 = 2$. Further process of deployment of outer corrugation of minimum diameter is possible only at forced increase of depth k of inner corrugation corresponding to it, by $\bar{\Delta} \leq a/2$ at the forming stage. It is obvious that after deployment of corrugation $n_{i/2}$ (Figure 4, a) transformation of undeformed surface of the shell by excess pressure is possible owing to compression of the technological caisson of volume V_K , satisfying the following condition:

$$V_K \geq V'_S. \quad (1)$$

Therefore, a criterion for complete deployment of the structure is r/R ratio meeting the same condition with preservation of shell isometricity at all the stages of transformation.

Figure 5 gives a schematic of a double-wall TSS for determination of ratios of conditional volumes of the interwall space (V_1, V_2, V_3, V_4) of the studied TSS, formed by revolution of ordinates of profiles of generatrices f_1, f_2, f_3, f_4

about the axis. Volume of interwall caisson V can be expressed as $V_2 + V_4 - V_3 - V_1$, or allowing for equality of inner volumes of the transformed shells $V = V_4 - V_3$. Congruence of generatrices of initial corrugated shells in any axial section of the structure at calculation of interwall caisson volumes allows their approximation by expressions for a cylindrical surface. Considering that $OA = BC = a$, one can write: $V = \pi a(R^2 - r^2)$. As condition (1) corresponds to relationship $\pi r^2 a \geq \pi a(R^2 - r^2)$, the ratio of double-wall TSS diameters required for complete deployment, will be expressed as

$$r \geq \frac{R}{\sqrt{2}}. \quad (2)$$

Combining double-wall TSS of a conical type into one structure by the respective bases of radii r and R allows producing a multicone TSS of a periodical profile, capable of deployment section-by-section at creation of excess pressure in the inner volume (Figure 6).

In this case, requirements to configuration of the interwall space and ratios of geometrical parameters expressed by relationships (1) and (2), remain the same. Design solution, which allows tightly joining the outer conical shells along the small radii, while providing the possibility of simultaneous deployment of the conjugated transformable surfaces, is shown in Figure 6, a and b. Leak-tightness and reciprocal mobility of contours K_1 and K_2 formed by the edges of radial holes in technological caisson covers of volume V_K (Figure 6, b) are provided by the compensating circular membrane with a fold, reversibly changing the deployment angle at transformation of each subsequent corrugation of double-wall TSS. Radii of contours K_1 and K_2 (R_{K1} and R_{K2}) are determined by design and technological considerations, whereas relationship (2) for a multicone TSS becomes $r_m = \sqrt{r^2 + R_K^2}$, where $R_K =$

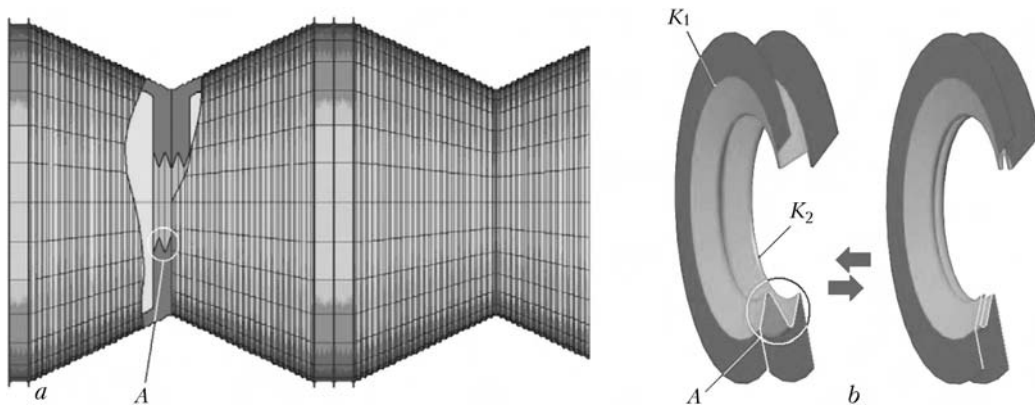


Figure 6. Construction diagram of multicone TSS of periodical profile (a), and compensating circular membrane (b) in the deployed and folded conditions (K_1, K_2 – radial contours associated with the inner and outer transformable shell of the structure, respectively): A – fold of compensating circular membrane

$= \frac{R_{K1} + R_{K2}}{2}$ is the average value of radius of circular membrane fold.

CONCLUSIONS

1. In the studied range of geometrical parameters of double-wall TSS the optimum structure is the one, in which the rectilinear and circumferential joints with different requirements to strength and ductility of welds are made by microplasma and laser welding processes.

2. Studied technology of producing permanent joints of austenitic stainless steel sheets allows ensuring the leak-tightness of deformable shells, both during forming, and at reverse transformation using excess pressure.

3. Complete transformation of double-wall TSS of a conical type up to design dimensions by creating excess pressure in the inner cavity, is possible with following of certain regularities of geometrical parameters on their inner and outer shells. Required ratios of working volumes of air in the structure interwall space are deter-

mined by relative values of radii of its bases, and are independent on the angle of conicity of the side surfaces at fulfillment of the condition of their isometricity.

4. The structure obtained by tight joining of double-wall conical TSS to each other preserves the functional properties of transformable elements included into it. The change of configuration of interwall gaps of each double-wall shell, associated with the need to unite the structure inner space into one volume, should be accompanied by fulfillment of the established dependencies of geometrical parameters in the connections.

1. (2003) *Space: technologies, materials, structures*. Ed. by B.E. Paton. Taylor&Francis.
2. Paton, B.E., Lobanov, L.M., Samilov, V.N. et al. (2006) Design and features of fabrication technology of a large-sized transformable shell structure. *The Paton Welding J.*, **7**, 2–10.
3. Shelyagin, V.D., Lukashenko, A.G., Garashchuk V.P. et al. (2011) Laser welding of thin-sheet stainless steel. *Ibid.*, **4**, 38–42.
4. Paton, B.E., Lobanov, L.M., Volkov, V.S. (2011) Transformable structures (Review). *Ibid.*, **12**, 25–33.

PECULIARITIES OF WEAR AND CRITERIA OF REPAIRABILITY OF DRILL BITS WITH DIAMOND-HARD-ALLOY CUTTERS

V.F. KHORUNOV, B.E. STEFANIV, O.M. SABADASH and V.V. VORONOV

E.O. Paton Electric Welding Institute, NASU, Kiev, Ukraine

The degree of wear and criteria of repairability of drill bits with diamond-hard-alloy cutters were studied. Statistical data on service life of different types of diamond drill bits were analysed.

Keywords: headway, mechanical speed, superhard materials, diamond layer, diamond-hard-alloy cutter (DHAC), wear resistance, drill well, polycrystalline diamond cutter (PCDC)

The rocks making up the well bore hole differ in composition and have different properties, depending on which the rocks can be destructed by cutting, spalling, abrasion or crushing. The character of fracture depends on the hardness and ductility of rock. Hence, drilling of wells is performed by using the certain type of tools. The main tool for mechanical destruction of rock to drill a well is a bit. Different types and kinds of bits are applied currently in practice.

The purpose of this study was to investigate peculiarities of wear and criteria of repairability of drill bits with DHACs.

The objects of the study are rotary drilling tools, such as bits, bores, various crowns and drill heads fitted with diamonds, hard alloys or diamond-hard-alloy materials in the form of cylindrical inserts. The drill bits and heads are made from strong and wear-resistant materials, as during the drilling process a bit is affected by axial loads, including impact ones, torque moment, as well as pressure and reactivity of a drilling mud.

In drilling, the initial shape of working surfaces of inserts changes due to wear, this leading to decrease in technical and economic indicators of the drilling tools. Abnormal wear and formation of circular grooves on the working surfaces of the bits make the tools unserviceable.

Wear of the working surfaces of drilling tools is a complex process caused by many factors,